Siderophore-Based Detection of Fe(III) and Microbial Pathogens

Tengfei Zheng and Elizabeth M. Nolan*

Department of Chemistry, Massachusetts Institute of Technology, Cambridge, MA 02139

*Corresponding author: lnolan@mit.edu

Phone: 617-452-2495

Fax: 617-324-0505

Abstract

Siderophores are low-molecular-weight iron chelators that are produced and exported by bacteria and fungi during periods of nutrient deprivation. The structures, biosynthetic logic, and coordination chemistry of these molecules have fascinated chemists for decades. Studies of such fundamental phenomena guide the use of siderophores and siderophore conjugates in a variety of medicinal applications that include iron-chelation therapies and drug delivery. Sensing applications constitute another important facet of siderophore-based technologies. The high affinities of siderophores for both ferric ions and siderophore receptors, proteins expressed on the cell surface that are required for ferric siderophore import, indicate that these small molecules may be employed for the selective capture of metal ions, proteins, and live bacteria. This minireview summaries progress in methods that utilize native bacterial siderophore scaffolds for the detection of Fe(III) or microbial pathogens.

I. Introduction

Iron is an essential nutrient for most organisms.[1-3] This first-row transition metal ion is involved in multiple biological phenomena essential to life that include oxygen transport and respiration, electron transfer, DNA synthesis and repair, and primary metabolism. Iron-containing enzymes also participate in secondary metabolism and the oxidative stress response. Iron is typically found in the +2 (ferrous) and +3 (ferric) oxidation states in biological systems, and higher oxidation states are achieved transiently during enzymatic catalysis. Organisms acquire this important nutrient by employing dedicated mechanisms for iron acquisition, transport, and storage.[2,4,5] Prokaryotes require micromolar (10^{-6} M) concentrations of iron to replicate and colonize, and are thus faced with a metabolic predicament because the concentration of Fe(III) at neutral pH is low (ca. 10^{-18} M).[6] Moreover, the free iron concentrations in living organisms, including the vertebrate host, are strictly regulated at lower concentrations (ca. 10^{-24} M in human serum)[6] because of the inherent toxicity of the metal ion, which results from its propensity cycle between the Fe^{3+}/Fe^{2+} oxidation states and generate deleterious radicals via Fenton chemistry. To acquire the concentrations of iron necessary to thrive in nutrient-limited environments, prokaryotes utilize a variety of strategies for iron acquisition.[2] Both Gram-negative and –positive bacteria produce and export siderophores (Figure 1),[7-9] a family of low-molecular-weight iron chelators, which are a focus of this minireview. Other tactics for iron acquisition include the uptake and utilization of heme iron,[10,11] which has been observed for *Staphylococcus aureus*, *Escherichia coli*, and *Mycobacterium tuberculosis,* and the expression of transferrin receptors on the cell surface, which allows various pathogenic species such as *Neisseriaceae* and *Pasteurellacea*, to obtain iron from host transferrin.[12,13] Acquisition of iron by these three mechanisms is associated with virulence.[9,11-16]

Siderophores comprise a family of low-molecular-weight iron chelators that are produced and exported by bacteria, fungi and plants, during periods of nutrient deprivation.[7,8] Most siderophores exhibit extraordinarily high affinity and selectivity for iron(III) with binding constants (K_a) ranging from 10^{30} M^{-1} to 10^{52} M^{-1} (Table 1).[17,18] Since mycobactin P was first isolated in 1949,[19] over 500 siderophores have been discovered, and approximately one half of these molecules have been characterized structurally.[7] Figure 1 presents siderophores **1**-**11**, which

highlight the structural diversity of this iron chelator family. Table 1 summarizes the producer organisms and iron affinities of select siderophores. With few exceptions (i.e. pyochelin **2**, *vide infra*), siderophores provide hexadentate coordination spheres for Fe(III) complexation and coordinate this metal ion with 1:1 stoichiometry. Figure 2 depicts ferrioxamine B,[20] Fe(III)-coordinated ferrichrome[21] and yersiniabactin,[22] and the vanadium(IV) complex of enterobactin.[23] Catecholates, hydroxamates, and α-hydroxycarboxylates are common bidentate ligands utilized by siderophores. Enterobactin is a canonical example of a triscatecholate scaffold whereas desferrioxamine and petrobactin are hydroxamate- and α-hydroxycarboxylate-utilizing siderophores, respectively. Heterocycles, formed via the enzyme-catalyzed cyclization of Ser and Cys building blocks,[24] provide basic nitrogen atoms and hence another strategy for iron coordination by siderophores as exemplified by pyochelin **2** and yersiniabactin **4**.

Nonribosomal peptide synthetase (NRPS) assembly lines are responsible for the biosynthesis of many siderophores.[8,24,25] The logic of these macromolecular machines has been covered elsewhere, and we direct the reader to comprehensive reviews on this topic for further information.[26,27] Siderophores are actively transported to the extracellular environment by dedicated export machinery. Following extracellular iron sequestration, the resulting ferric-siderophore complexes are captured by specific membrane receptors (K_d values are typically in the nanomolar range), providing a means for iron uptake.[28-30] The structures and mechanisms of siderophore uptake machinery vary for Gram-negative and –positive bacteria. Gram-negative bacteria have a double-layer membrane structure,[31] and utilize an outer membrane receptor, a periplasmic binding protein, an inner membrane ABC transporter, and the TonB complex for ferric siderophore transport. The TonB complex controls the transfer of the siderophore from the outer membrane receptor to the periplasm binding protein, and the ABC transporter provides cytoplasmic entry.[32,33] Less is known about the siderophore uptake process in Gram-positive bacteria; these species express lipoproteins and ABC transporters that may be responsible for ferric-siderophore transport.[2,34] Both the biosynthesis and transport of siderophores are regulated by repressor proteins that are sensitive to iron concentration. For example, Fur is the iron-uptake regulation protein expressed by most Gram-negative bacteria. Fur is a Fe(II)-binding

protein, and the holo form coordinates to specific DNA regulatory sequences, thereby repressing the transcription of relevant genes when iron levels are high.[35,36]

Comprising a family of important natural products with fascinating structural features, total syntheses of many siderophores have been achieved, providing entry points into modification of these intriguing scaffolds for various applications. One established medicinal use of siderophores and synthetic siderophore mimics is in the treatment of iron-overload diseases including hemochromatosis and thalassemia.[37,38] Desferrioxamine B is an FDA-approved iron chelator for the treatment of such diseases. Along these lines, siderophores and siderophore mimics also have potential as cancer therapeutics because cancer cells require high concentrations of iron for proliferation.[39,40] Starving cancer cells of iron using siderophore-based compounds is therefore of interest for cancer therapy. Another active research area is the design and application of siderophore-drug conjugates.[41] This work is largely inspired by a family of naturally-occurring siderophore-antibiotic conjugates called sideromycins, which includes the *Streptomyces* natural product albomycin.[42,43] These remarkable secondary metabolites serve as "Trojan horse" antibiotics that are recognized and transported into recipient bacterial cells by siderophore uptake machinery. Applying the same strategy, a range of synthetic siderophore-antibiotic conjugates have been designed, synthesized, and evaluated for antibacterial activity.[44-47] These conjugates generally exhibit β-lactams, fluoroquinolones, sulfonamides, and other small-molecule drugs coupled to hydroxamate- and catechol-based siderophores or siderophore-inspired molecules. A mycobactin-artemisinin conjugate was reported recently and exhibits activity against *Mycobacterium tuberculosis* and the malaria pathogen.[48]

From the standpoints of therapeutic and analytical potential, siderophores hold significant promise. With a focus on the latter arena, the following sections of this minireview summarize siderophore-based strategies for Fe(III) sensing and pathogen detection. In both cases, the exquisite specificity and high affinity of a siderophore for ferric ion or its receptor provide the basis for using these molecules as sensors or probes. In Section II, we review siderophore-based iron detection with focus on fluorescent molecules. This sensing sub-discipline is established, but has received less critical review than other areas of fluorescence-

based metal-ion sensing.[49-51] Fluorescence probes incorporating siderophore scaffolds that provide rapid, selective and sensitive responses to Fe(III) hold significant promise for investigating iron uptake by siderophore-utilizing organisms and, more broadly, the roles of iron in biology with particular emphasis on the so-called labile iron pool.[52,53] These tools are also useful for monitoring iron concentrations in environmental and clinical samples. In Section III, we cover developing technologies that provide siderophore-based pathogen capture.[54-56] These proof-of-concept studies are motivated by a need for rapid and reliable methods for detecting virulent bacteria in food products, the environment, and in clinical samples. We intend for this review to complement prior reviews that address siderophore coordination chemistry,[18,57] siderophore-based chelation therapy,[37,38] siderophores and cancer therapy,[39,40,58] and siderophore-antibiotic conjugates for drug delivery.[41,44-47,58] We chose to limit the scope of this minireview to platforms that utilize native siderophore scaffolds rather than siderophore mimics. A wealth of literature pertaining to the design, synthesis, and application of siderophore analogs exists,[59-72] some of which has been reviewed recently,[18] and we note that a number of these molecules are fluorescent Fe(III) sensors.[65-72]

II. Strategies for Fe(III) Detection

In this section, we highlight select examples where naturally-occurring siderophores have been employed for the detection of Fe(III) by using fluorescence. We first consider naturally-emissive siderophores, including pyoverdines (i.e. **1**) produced by *Pseudomonas* spp. and azotobactin **3** from the soil bacterium *Azotobacter vinelandii*.[9,73-83] Next, we evaluate several synthetic fluorophore-siderophore conjugates where fluorophores are attached to native siderophore scaffolds to provide fluorescence responses following Fe(III) coordination.[84-88] Iron is a paramagnetic metal ion and thus has a propensity to quench fluorophore emission. As a result, most of the siderophores described herein afford fluorescence quenching or “turn-off” following Fe(III) recognition. Lastly, we present a lanthanide-based approach where Fe(III) coordination results in lanthanide displacement and loss of lanthanide luminescence.[89]

II.a. Fe(III) Detection Based on Naturally-Emissive Siderophores

Among the most celebrated fluorescent siderophores are the pyoverdines (i.e. **1**),[90] which are produced by all fluorescent pseudomonads including *Pseudomonas aeruginosa* and *P. fluorescens*, and the nitrogen-fixing soil bacterium *Azotobacter vinelandii*. The PVD gene cluster of *Pseudomonas* spp. is responsible for the biosynthesis of pyoverdines.[91] These nonribosomal peptides are comprised of a N-terminal dihydroxyquinoline chromophore, a peptide arm of six to twelve residues in length, and a side chain that is most often a small dicarboxylic acid or amide (Figure 1).[90] The length and composition of the peptide arm are highly variable and strain-specific. Both L- and D-amino acids, in addition to a number of unusual monomeric building blocks such as hydroxaspartate and N^{δ}-hydroxyornithine, comprise the peptide arms. Over fifty pyoverdines or pyoverdine-like natural products have been isolated and structurally characterized.[92] Pyoverdines form hexacoordinate Fe(III) complexes ($K_a \sim 10^{29}$ M^{-1}) and bind iron by using both hydroxamate and catecholate groups. Other emissive siderophores include azotobactins (i.e. **3**),[93,94] pyochelin **2**,[95] and scaffolds containing spermidine (i.e. parabactin, **8**) or other groups that emit light, albeit weakly. In this section, we describe examples where a naturally-occurring siderophore has been employed for Fe(III) detection. In all cases, the siderophores were isolated and purified from cultures of the producing organism and iron coordination results in quenching or "turn-off" of siderophore emission. We first consider fluorescent siderophores employed for Fe(III) sensing in solution.[73-75] Subsequently, we describe efforts to immobilize siderophores in materials, including micelle-templated silica and sol gel, for the optical detection of this metal ion.[76-81,83]

Azotobactin δ **3** is a fluorescent siderophore produced by *Azotobacter vinelandii* and shares structural similarities with the pyoverdines. In the laboratory, this natural product can be isolated in quantities of 100 – 200 mg/L of culture when a mutant strain that overproduces the siderophore is employed,[96,97] providing sufficient quantities for extensive analytical work. Azotobactin δ is comprised of a decapeptide, (L)-Asp-(D)-Ser-(L)-Hse-Gly-(D)-*β-threo*-HOAsp-(L)-Ser-(D)-Cit-(L)-Hse-(D)-N^{δ}-Acetyl, N^{δ}-HOOrn-(L)-Hse lactone, appended with an N-terminal 6,7-diamino-2,3-dihydroxyquinoline chromophore (Figure 1; Hse, homoserine; HOAsp, hydroxyaspartic acid; Cit, citrulline; HOOrn, hydroxyornithine). Azotobactin δ utilizes the

hydroxamate group of N^{δ}-Acetyl, N^{δ}-HOOrn, the α-hydroycarboxylic moiety of *β-threo*-HOAsp, and the dihydroxyquinoline-derived catechol group to coordinate Fe(III).[74] The optical absorption spectrum of azotobactin δ in aqueous solution at pH 5 exhibits a maximum at 380 nm (ε = 23,500 $M^{-1}cm^{-1-}$) and a shoulder at 336 nm (ε = 19,600 $M^{-1}cm^{-1}$). Addition of Fe(III) to solutions of azotobactin δ results in a red-shift in the wavelength of maximum absorption to 412 nm (ε = 23,000 $M^{-1}cm^{-1}$) with shoulders at 450 (ε = 10,000 $M^{-1}cm^{-1}$) and 550 nm (ε = 2,000 $M^{-1}cm^{-1}$). The shoulders are attributed to LMCT originating from the dihydroxyquinoline-based catecholate and hydroxamate binding sites. The stability constant for the ferric azotobactin δ complex was first reported to be ca. 10^{30} M^{-1} from thermodynamic analysis,[73] and subsequent kinetic analyses and potentiometry from the same research group provided a value of 1.9 x 10^{-10} M^{-5}.[74]

Azotobactin δ provides maximum emission at 490 nm (λ_{ex} = 380 nm) in acetate buffer (pH 4.4). Addition of one equivalent of Fe(III) to solutions of azotobactin δ causes fluorescence turn-off and a slight blue-shift in the wavelength of maximum absorption.[73] The quantum yield for azotobactin is 0.28 at pH 2 (6-hydroxypyrene-1,3,6-trisulfonic acid standard; Φ = 0.96, pH 2).[97] A fluorescence assay for Fe(III) determination using azotobactin δ provided a linear range between 0 – 95 ng/mL Fe(III) and a detection limit of 0.5 ng/mL (89 nM; acetate buffer, pH 4.4).[73] The emission readout from this assay was not perturbed by Na(I), Ca(II) or Mg(II) (2 to 5 x 10^3-fold higher concentrations than that of ferric ion) whereas low concentrations of Cu(II) and Al(III) compromised the Fe(III)-induced response.

A fluorescence method employing azotobactin as an Fe(III) reporter was subsequently devised for quantifying non-transferrin-bound iron (NTBFe) in the serum of thalassemia patients.[75] Thalassemics suffer from iron overload and concentrations of NTBFe can reach 10 μM in the serum of these patients. This disease is prevalent in developing countries, motivating the development of facile and inexpensive detection methods for monitoring NTBFe levels. This azotobactin-based approach involves (i) saturation of any apo transferrin in the serum by Co(III) addition, (ii) mobilization of non-transferrin-bound iron by using nitrilotriacetic acid, (iii) removal of all serum proteins, and (iv) addition of azotobactin to the resulting solution to quantify Fe(III) by using a calibration curve prepared with iron-spiked serum from healthy human subjects. Samples from sixty-three thalassemics were analyzed by this assay, which provided Fe(III)

concentrations in the range of 0.07 – 3.24 μM. These values correlated with serum iron levels and percent transferrin saturation, and also with colorimetric determination of Fe using the established bathophenanthrolinedisulfonate (BPT) method. It should be noted that fluorescence-based assays for NTBFe using synthetic siderophore-fluorophore conjugates[98] and fluorophore-modified iron-binding proteins[99] have been reported and reviewed elsewhere.[52] In general, fluorescence-based techniques have the advantages that iron concentrations can be monitored rapidly on-site and without the need for sophisticated instrumentation (i.e. inductively coupled plasma mass spectrometry or atomic absorption spectroscopy); however, one drawback is that serum/sample color and also sample turbidity are oftentimes variable and may interfere with the fluorescence measurements.

Fluorescent siderophores also find application in assays designed for either monitoring Fe(III) levels in water samples, and in technologies for waste water treatment. The tactics highlighted below all involve the encapsulation or immobilization of a fluorescent siderophore into a material, which thereby sequesters iron from the aqueous phase. In many instances, these materials are incorporated into flow cells and afford rapid quantification of Fe(III), and are recyclable. Such portable Fe(III) detectors are amenable for work in the field, which includes the rapid analysis of environmental samples and potentially quick clinical diagnostics. Most of the examples described below utilize pyoverdine (i.e. **1**). Pyoverdine exhibits high water solubility, forms a 1:1 complex with Fe(III),[100] and exhibits maximum emission at ca. 450 nm in solution. Like azotobactin δ, pyoverdine affords a turn-off fluorescence response to Fe(III). Pyoverdine has been immobilized on controlled pore class (CPG), in large-pore micelle-templated silica (MTS), and in sol gels for Fe(III) detection.[76-79]

In the early 1990s, pyoverdine was immobilized on CPG and thereby incorporated into a flow cell, which provided iron determination in the 10 – 200 ng/mL range and a modest detection limit of 3 ng/mL.[76] This approach was employed to evaluate iron concentrations in tap and mineral waters, and the resulting data were in agreement with data obtained by inductively coupled plasma atomic emission spectroscopy (95% confidence level). Because acidification results in catechol protonation and release of Fe(III) from pyoverdine, the flow cell was regenerated by flushing with 1 M HCl, and longevity studies revealed that an individual cell had

a lifetime of ca. three months or one-thousand measurements. Subsequently, this method was modified to for the analysis of iron speciation by outfitting the flow cell with a column containing persulfate.[77] When the column was bypassed, the flow cell only reported on Fe(III). Flowing the solution of interest through the persulfate column resulted in oxidation of any Fe(II) to Fe(III) and thereby provided a measurement of total dissolved iron. This particular system was employed to determine total iron levels in tap water, well water, and wine. Like the first-generation sensor, this system was used repeatedly over the course of three months. Ten to fifteen samples may be processed each hour.

A related tactic is to encapsulate or immobilize pyoverdine in MTS.[78,79] A direct synthetic procedure was first devised where pyoverdine was dissolved in the templating micelles, and the resulting MTS provided reversible fluorescence quenching with Fe(III) addition.[78] This preparation, however, resulted in insufficient encapsulation of the pyoverdine and alternative immobilization strategies were subsequently pursued. Along these lines, pyoverdine was covalently attached to a glycidoxy-grated large-pore MTS and a commercial high-grade glycidoxy-grafted silica gel (Figure 3).[79] These materials served as metal ion sponges and sequestered iron from solutions containing mixed metal samples. In some instances, chromium interference was observed. Pyoverdine was also entrapped in sol-gel glass for Fe(III) detection.[81,83] In one case, the siderophore exhibited maximum emission at 405 nm when encapsulated in the sol-gel, and maximum intensity was observed in the pH 5 to 7.5 range. [81] Pyoverdine retained its Fe(III)-induced turn-off fluorescence response in the sol gel, and these Fe(III)-responsive materials exhibited greater stability than the CPG-based systems described above. The detector was employed to analyze iron concentrations in Madrid tap water and human serum.[81]

Lastly, the intrinsic emission of parabactin (**8**, Figure 1) has been employed for the detection of bioavailable Fe(III) in ocean waters.[82] Parabactin is a spermidine catecholate siderophore produced by *Paracoccus denitrificans* that employs two catechol moieties and a 2-(2-hydroyxl)oxazoline to form a wine-colored hexacoordinate iron complex with a K_a value of 10^{48} M^{-1} at basic pH.[101] In ethanol and in aqueous solution adjusted to pH 3.1, parabactin exhibits three absorption bands centered at 210, 250 and 311 nm. The latter two absorption

bands red shift to 253 and 316 nm at pH 8. Addition of Fe(III) to solutions of parabactin results in a new absorption feature centered at 500 nm (10 mM tricine buffer, pH 8). The emission spectrum of apo parabactin also exhibits solvent- and pH-dependence; the wavelength of maximum emission is observed at 401 (ethanol), 440 (pH 3.3) or 460 nm (pH 8.0) following excitation at 311 nm. Addition of Fe(III) to solutions of parabactin results in fluorescence quenching. To provide a recyclable biosensor for Fe(III) determination in ocean waters, parabactin was added to a sol-gel solution and the mixture was spin coated onto quartz.[82] The encapsulated parabactin exhibited absorption and emission properties similar to those observed for free parabactin at pH 3.1, which was attributed to an acidic microenvironment in the pores resulting from the acid-catalyzed preparation of the sol gel. A flow cell was outfitted with the sol gel, and parabactin emission turned off when aqueous Fe(III) was flushed through the devise. Using this Fe(III)-dependent fluorescence change, an Fe(III) calibration curve was prepared (0.05 to 1 nM) and a detection limit of 40 pM for Fe(III) achieved, the latter of which is impressive given that the emission from parabactin is not especially bright as judged by the chromophore (Φ and ε values were not reported in this work). To further evaluate this strategy, the Fe(III) content in a standard seawater reference sample was determined to be 3.24 ± 0.35 nM, in good agreement with the certified value of 3.71 ± 0.63 nM. Next, seawater samples collected from varying depths (3 to 303 m) in the North Atlantic Ocean (49^{o}38.0'N, 18^{o}31.8W) were analyzed, and the parabactin-derived biosensor reported that iron concentrations vary from <100 pM in surface waters to 700-1000 pM at a depth of 300 m. This concentration range is similar to those reported by others studying iron concentration gradients in the North Atlantic Ocean.[102]

II.b. Fe(III) Detection Based on Synthetic Fluorophore-Siderophore Conjugates

A complementary approach to siderophore-based optical detection of Fe(III) is to modify naturally-occurring siderophores with synthetic fluorophores, affording siderophore-fluorophore conjugates that provide changes in emission following Fe(III) coordination. This tactic requires that the siderophore has a functional group amenable to synthetic modification, and that fluorophore conjugation has negligible impact the iron-binding properties of the chelate. To date,

the DFO and pyochelin scaffolds have been utilized for the assembly of Fe(III)-responsive siderophore-fluorophore conjugates (Figures 4-6).[53,84-86,88,103] The DFO conjugates **12**-**16** (Figures 4 and 5) provide turn-off sensing of Fe(III) whereas fluorescence enhancement or "turn-on" detection of this metal ion is achieved with the pyochelin conjugates **17**-**18** (Figure 6). Advantages of employing DFO include its commercial availability and its N-terminal amino group, the latter of which is a synthetic handle for fluorophore attachment. Preparation of the pyochelin-fluorophore conjugates required multistep syntheses, and these routes provide access to a multitude of other pyochelin-based molecules.[104]

II.b.i. DFO-Fluorophore Conjugates for Turn-Off Fe(III) Detection

DFO, **5**, is a hydroxamate-based siderophore produced by the soil actinomycete *Streptomyces* (Figure 1). Although it is the first and only FDA-approved siderophore drug for treating iron-overload disease, the lack of oral availability and low cell permeability limit its utility. In the early 1990s, a derivative of DFO bearing a terminal nitrobenz-2-oxa-1,3-diazole (NBD) moiety was reported (**12**, NBD-DFO, Figure 4).[84] NBD-DFO is water-soluble, exhibits maximum emission centered at 548 nm (λ_{ex} = 475 nm), and affords fluorescence quenching upon addition of Fe(III) (10 mM HEPES, 100 mM NaCl, pH 7.4). Mixtures of acid (pH < 5) and excess EDTA reverse Fe(III)-induced turn-off, confirming that NBD-DFO is a turn-off Fe(III) sensor and that the fluorophore-modified chelate retains a high-affinity for this metal ion. A stability constant for NBD-DFO for Fe(III) was not reported and is assumed to be similar to that of parent DFO (Table 1). Negligible changes in apo NBD-DFO emission occur following addition of Ca(II) and Mg(II) whereas Mn(II), Zn(II) and Cu(II) afford variable degrees of fluorescence quenching. The turn-off behavior induced by Mn(II) and Zn(II) is only observed with excess metal ion (100 to 200-fold greater than ferric ion). In contrast, introduction of one equivalent of Cu(II) into solutions of NBD-DFO results in quenching. The copper-induced fluorescence decrease is reversible by addition of acid, suggesting a means of differentiating a turn-off response generated by Cu(II) or Fe(III) by using acid and acid/EDTA mixtures.

NBD-DFO was subsequently employed in two biological contexts.[84,85] In one report, the anti-plasmodium activity of NBD-DFO was evaluated.[84] DFO itself suppresses malarial infection

in vitro and in several rodent/primate species *in vivo*, but exhibits slow penetration into erythrocytes, which hinders its therapeutic utility. NBD is relatively lipophilic and NBD-DFO lacks the terminal amino group of the parent compound, suggesting that this fluorophore modification may result in improved cellular uptake and more potent inhibition of *P. falciparum* growth. The ability of NBD-DFO to inhibit intraerthyrocytic *P. falciparum* growth was therefore investigated. Dose-response studies revealed an IC_{50} value of 5 +/- 0.62 μM. This value is 5-to-6-fold lower than the IC_{50} value of unmodified DFO (26 +/- 5 μM). Apo NBD-DFO uptake experiments employing uninfected and infected erythrocytes monitored by NBD emission suggested that the uptake was highly selective for the infected cells. Complementary uptake studies employing radiolabeled ^{59}Fe-NBD-DFO revealed that the negligible cellular entry of iron-bound form.

NBD-DFO was subsequently utilized to monitor iron uptake in maize and cotton roots.[85] Radiolabeled ^{55}Fe-NBD-DFO was transported into both maize and cotton roots that were cultured in iron-deficient media. A time-dependent fluorescence increase in both the cotton and maize roots treated with Fe-bound NBD-DFO was observed over ca. fifteen hours by fluorescence microscopy. The magnitude of fluorescence enhancement was greater for roots that were cultured in iron-deficient media compared to those supplemented with 100 μM FeEDTA. Because NBD-DFO binds Fe(III) reversibly, one possible explanation for the observed fluorescence enhancement is iron release from NBD-DFO and hence the monitoring of intracellular siderophore dynamics and iron utilization. Other explanations include (i) uptake of ferric NBD-DFO because the observed fluorescence increase results from weak emission from this coordination complex and (ii) instability of the probe manifest as photoactivation.

Fluorescein-derivatized DFO conjugates (**13,** FL-DFO_{thio}; **14**, FL-DFO_{am}, Figure 4) have also been reported.[52,53,86,87] These particular siderophore-fluorophore conjugates are appealing from the photophysical perspective because fluorescein exhibits high brightness (Φ x ε) and water compatibility.[105] Compounds **13** and **14** each exhibit a fluorescein moiety coupled to the N-terminal amine of the siderophore, provide turn-off Fe(III) sensing in aqueous solution, and are biologically compatible. Sensor **13** was once commercially available from Molecular Probes, Inc. (now Invitrogen) and has been employed to measure levels non-transferrin-bound iron in serum.[98,99] One assay measured desferrioxamine-chelatable iron (DCI) in serum, which can be

used as an efficiency index of a chelation therapy. Patients treated with deferiprone, an iron-chelating drug, showed substantial increase of DCI after two hours of oral administration. Deferiprone has much better cell permeability than DFO. The results of this study indicated that deferiprone shuttles intracellular iron to extracellular DFO, suggesting a new chelation therapy by using a combination of deferiprone and DFO. In another recent application, FL-DFO_{am} **14** was immobilized onto mesoporous silica to provide highly selective and sensitive iron nanosensors.[86] The optimized sensor, which exhibited minimal FL-DFO_{am} leaching, was prepared by covalently anchoring FL-DFO_{am} to the amine-functionalized internal surface of the mesoporous silica material. This hybrid material can be compressed into small pellets, which exhibit a linear response to Fe(III) concentrations in the low-micromolar range when incubated in solutions containing this metal ion. Selectivity studies showed that Ca(II), Al(III), and Ni(II) do not interfere with the response, and Cu(II) partially quenches the sensor emission. Further development of this approach may provide portable and stable iron nanosensors with high sensitivity and selectivity for use in the field.

The last examples of fluorophore-DFO conjugates that provide fluorescence quenching with Fe(III) coordination are **15** and **16**, the former of which was designed for tumor imaging and treatment (Figure 5).[87] Multifunctional conjugate **15** is comprised of a near-infrared (NIR) fluorescent moiety (cypate), a cyclic peptide (RGD) for receptor-specific recognizing and cellular internalization, and the DFO moiety. The RGD peptide binds the integrin $\alpha_V\beta_3$ receptor (ABIR). This receptor is overexpressed on the endothelial cells in many tumors and therefore is a target for tumor imaging, diagnosis, and therapy. An in vitro study using ABIR-positive cells revealed that incorporation of RGD peptide improved the cellular uptake of DFO, and the conjugate remained in the cellular space for up to 10 h. Cellular distribution studies showed that compound **15** accumulated in the mitochondria, lysosomes and the cytosol. Further studies addressing intracellular iron chelation by the probe may afford insights about iron-related molecular-recognition processes.

II.b.ii. Pyochelin-Fluorophore Conjugates for Turn-On Fe(III) Detection

Pyochelin (**2**, Figure 1) is a yellow-green emissive siderophore that was first isolated from *Pseudomonas aeruginosa* cultures in the late 1970s.[106,107] In contrast to the siderophores discussed thus far, pyochelin contains neither catecholate nor hydroxamate groups. It is a tetradentate ligand that coordinates Fe(III) via one phenolate and one carboxylate oxygen atom, and two nitrogen atoms from thiazoline and thiazolidine heterocycles. Pyochelin forms 1:1 and 1:2 Fe:L complexes, with the second pyochelin proposed to coordinate in a bidentate fashion, and exhibits relatively low Fe(III) affinity compared to other siderophores (Table 1).[106,108] Pyochelin also forms coordination complexes with Co(II), Ni(II), Cu(II), and Zn(II) and Mo(VI).[109] Because of its unusual structure, relatively weak Fe(III) affinity, and the relatively low levels of pyochelin produced by *Pseudomonas* cultures, this natural product has been described by some as a "secondary siderophore."[90]

Two pyochelin-NBD conjugates, **17** and **18**, that provide fluorescence enhancement following Fe(III) coordination in aqueous solution were reported recently (Figure 6).[88] These sensors differ from one another in the nature of the linker installed between the siderophore and fluorophore moieties. Sensor **17** exhibits a relatively short succinate linker whereas a long and flexible polyethyleneglycol moiety is incorporated into **18**. In both molecules, the linker is connected to pyochelin via the N3" position, which is involved in iron coordination. The syntheses of **17** and **18** involved eleven and twelve steps, respectively, and both molecules retained iron-coordinating ability. Addition of Fe(III) to aqueous solutions of **17/18** resulted in fluorescence enhancement centered at 545 nm (150 mM Tris buffer, pH 8). Five equivalents of Fe(III) were required for maximum turn-on with 2.9- and 3.2-fold emission enhancement observed for **17** and **18**, respectively. This turn-on behavior is in striking contrast to the fluorescence quenching observed for unmodified pyochelin following Fe(III) coordination.[95,106] Job plot analyses indicated 1:2 and 1:3 Fe:L stoichiometries for **17** and **18**, respectively. Neither selectivity of **17/18** for Fe(III) over other first-row transition metal ions nor whether the fluorescence turn-on is specific for Fe(III) were reported, and future studies along these lines are warranted. Fluorescence microscopy studies employing *P. aeruginosa* PAD07, a strain expressing the pyochelin receptor FptA, indicated that FptA binds and transports **17**.

Intracellular fluorescence from the NBD chromophore was observed. In contrast, no cellular labeling was observed for *P. aeruginosa* DH51, which does not express FptA, following incubation with **17**. These preliminary experiments indicate that **17** is suited for studying pyochelin uptake in *Pseudomonas* and other organisms, and that FptA may transport various pyochelin-derivatized cargos.

To date, few turn-on fluorescent detectors for Fe(III) have been reported,[49,72,110-112] making these pyochelin-fluorophore conjugates important contributions to the broad field of metal-ion sensing. Moreover, several of the turn-on Fe(III) sensors reported to date have relatively low affinity (K_d ~ 5 – 300 μM) and hence high detection limits, which limit practical utility.[49] Unraveling the photophysical properties of the apo and iron-bound forms of **17**/**18**, and precisely how the synthetic modifications at the N3" position influence the coordination behavior of pyochelin, will be enlightening and provide insight for the design of second-generation turn-on pyochelin-based metal-ion sensors in addition to other types of pyochelin-based conjugates.

II.c. Fe(III) Detection Based on Lanthanide Displacement

Several displacement approaches for metal-ion detection have been reported and afford either a turn-on or turn-off fluorescence response to the metal ion of interest. Frequently, a metal ion that shares the same coordination site as the analyte and substantially quenches background emission from the receptor is employed. Displacement of this metal ion by the analyte results in fluorescence enhancement that is not achieved by using the receptor alone. This particular strategy has been utilized for turn-on Hg(II) sensing by Cu(II) displacement from a naphthlene-derivatized dihydrazone ligand,[113] and for improving the dynamic range of the turn-on Zn(II) sensor Zinpyr-1 (ZP1) by substituting the Mn_2:ZP1 complex for apo ZP1 as the Zn(II) probe.[114] A complementary displacement tactic requires a lanthanide ion, the luminescence of which provides an indirect spectroscopic probe of the metal ion of interest following displacement of the antenna[115] or the lanthanide ion itself. The latter strategy was recently employed for turn-off Fe(III) detection using terbium-bound *N*-methylanthranyl desferrioxamine B (**19** and **20**, Figure 7).[89]

Lanthanide ions coordinate to hydroxamate, catecholate, and salicylamide ligands, and siderophores have been proposed to mediate actinide mobility in contaminated subsurface environments.[116,117] DFO B, **5**, prevents Eu(III) absorption by goethite (α-FeOOH) and boehmite (γ-AlOOH), at least under laboratory conditions.[118] The possibility of employing lanthanide complexes of *N*-methylanthranyl DFO B for Fe(III) detection was likely inspired, at least in part, from such prior studies. It was hypothesized that the *N*-methylanthranyl moiety would serve as the antenna and thereby transfer energy to the coordinated Ln(III) ion, providing luminescence. Following excitation of **19** at 340 nm, Tb(III) emission was observed in organic solvents such as ethyl acetate and acetonitrile. Addition of Fe(III) to a solution of **19** in ethyl acetate resulted in luminescence quenching, attributed to displacement of Tb(III) from the chelate and formation of **21**. A detection limit for Fe(III) was not provided for this siderophore-based detector, and the Tb(III) emission was quenched in protic solvents, including methanol and methanol/water mixtures, which limits its utility. A β-diketonate derivative of Tb:MA-DFB, **20**, was next prepared by using hexafluoroacetylacetone (Hfac) as a blocking ligand to prevent water molecules from binding to the Tb(III) center. This β-diketonate complex exhibited Tb(III) emission in water, which was quenched following addition of Fe(III). A detection of 5 nM in water was reported; however, compound **20** was not tested in more complex or real-world samples. From the standpoint of design, the choice of Hfac as a blocking ligand over other β-diketones known to enhance Tb(III) luminescence is unclear, and systematic variation of the β-diketone may prove to be worthwhile for tuning the luminescence properties of the Tb(III) complex.[119] Further studies will reveal whether such siderophore-based, Fe(III)-induced lanthanide displacement approaches are applicable to other siderophore scaffolds and have practical utility.

III. Strategies for Pathogen Detection

In this section, we present four recent strategies for or applicable to the detection of microbial pathogens that require siderophores.[54-56,120] These methods rely on siderophore immobilization and take advantage of the high-affinity association of siderophores to bacterial cell-surface receptors. Following iron coordination, ferric siderophores are recognized and sequestered by dedicated uptake machinery expressed on the cell membrane (Section I), which

provides a route for cytoplasmic entry. A number of siderophore receptors have been characterized structurally and biochemically with prominent examples including FepA[121] (enterobactin receptor) and FhuA[122] (ferrichrome receptor) of *E. coli*, and FpvA[123] (pyoverdine receptor) of *Pseudomonas aeruginosa* among others. These receptors exhibit specificity for one or several siderophores and bind these small molecules with dissociation constants in the nanomolar range. This specificity, in addition to the high-affinity binding capacity of the siderophore receptors, is attractive for developing species-specific bacterial identification and capture technologies. Moreover, from the perspective of pathogen detection, targeting siderophore receptors is worthwhile because the expression of functional siderophore uptake pumps is essential for proliferation and virulence in the iron-limiting environment of the vertebrate host. The likelihood of pathogens mutating these receptors is low.

A recent proof-of-concept example of siderophore-based pathogen detection involved polydimethylsiloxane (PDMS) stamping and immobilization of pyoverdine onto gold-plated glass chips for the capture of the opportunistic human pathogen *Pseudomonas aeruginosa* (Figure 8).[54] FpvA is the pyoverdine receptor expressed by *P. aeruginosa* and it has a K_d value of ca. 0.5 nM for its iron-bound ligand.[124,125] Pyoverdine was complexed with gallium and coupled to bovine serum albumin (BSA) by using carbodiimide chemistry. Subsequently, a PDMS stamp housing a pattern of repeating parallel ridges was treated with pyoverdine-BSA and employed to imprint a parallel pattern of pyoverdine-BSA onto gold-plate glass chips. In the first set of experiments, the chips were treated with solutions of DiO-labeled *P. aeruginosa* and the resulting emission pattern was visualized by using fluorescence microscopy. DiO, 3,3'-dioctadecyloxacarbocyanine perchlorate, is a commercially-available fluorescent dye that binds to cell membranes. These experiments revealed a parallel pattern of DiO emission, with emission corresponding to the pyoverdine-functionalized regions of the chip. This pattern indicated that *P. aeruginosa* bound to the chip only where pyoverdine was attached. Because pre-loading the bacteria sample with a fluorophore is impractical for achieving rapid pathogen detection in real-world samples, the DiO-labeling step was ultimately circumvented by using light scattering, followed by Forrier transform analysis, to visualize the siderophore-captured bacteria. Using this technique, 10^4 cells/mL were routinely detected. In some instances, *P.*

aeruginosa from cultures at 10^2 cells/mL was observed. Only fifteen minutes were required for maximum *P. aeruginosa* binding, making this approach significantly more rapid compared to established methods for pathogen detection such as PCR-based screens.

To probe the selectivity of the pyoverdine-modified chips for pyoverdine-producing organisms, the chips were treated with *E. coli* or *Yersinia enterocolitica*, species that neither express FpvA nor utilize pyoverdine for iron acquisition. Only negligible patterning was observed, supporting a requirement of a pyoverdine receptor for chip-based detection. It should be noted that the effect of metal-ion coordination by pyoverdine on the detection limit was not addressed in this study. It is unclear whether the pyoverdine stamped onto the gold chips is gallium-bound, iron-coordinated (resulting from iron-induced displacement of gallium), metal-free or a mixture of these species. Although iron-free and gallium-bound pyoverdine bind to FpvA,[124,126] the speciation may influence the detection limit for this system or for similar chips that utilize different siderophores.

Following this proof-of-concept report, the siderophore-modified chip methodology was extended to the detection of *Yersinia enterocolitica*.[55] This Gram-negative human pathogen causes gastroenteritis and employs its xenosiderophore DFO (**5**, Figure 1) for iron acquisition. The receptor FoxA is responsible for ferrioxamine uptake by *Y. enterocolitica*,[127,128] and utilization of this siderophore is associated with virulence and systemic infection in patients receiving chelation therapy for iron overload.[129] A ferrioxamine-BSA conjugate was therefore prepared by using carbodiimide chemistry, and a PDMS stamp was treated with ferrioxamine-BSA and used to pattern a gold-plated glass surface. The chips were subsequently incubated with 10^8 CFU/mL of *Y. enterocolitica*, which grown under iron-deficient conditions, and analysis of the chips revealed a light-scattering pattern attributed to pathogen capture. This pattern was not observed for chips treated with unmodified BSA or when the cultures of *Y. enterocolitica* were pretreated with desferrioxamine to saturate FoxA. LIVE/DEAD staining indicated that >95% of chip-bound bacteria were alive, and incubation of the chips with dead *Y. enterocolitica* resulted in no patterning. As observed for the pyoverdine-modified chips, signal saturation was observed following a ca. fifteen-minute incubation (10^8 cells/mL). Optimized chips, bearing a 20-30% weight ratio of siderophore/BSA, afforded a detection limit of 10^3 CFU/mL observable by

the eye. The chips retained *Yersinia* capture ability after one year of storage. To evaluate the selectivity of the chips for ferrioxamine-utilizing microbes, the chips were treated with *Staphylococcus aureus*, *Mycobacterium smegmatis*, *Pseudomonas aeruginosa*, and *Vibrio cholerae*. Negligible to no pathogen capture was observed for cultures of *S. aureus*, *M. smegmatis*, and *P. aeruginosa* whereas *V. cholerae* was bound by the chips. An experiment testing chip performance with a mixed species sample was not reported. Nevertheless, these results point to a need for multiplexing and incorporating orthogonal siderophores on a given chip for rapid species-specific identification in mixed bacterial samples.

Siderophore-modified CdSe/ZnS quantum dots (QDs) were employed to capture *Pseudomonas fluorescens* previously isolated from the Dong-Hu Lake in China.[56] *P. fluorescens* is typically found in soils and waters, and this bacterium produces the fluorescent siderophores pyoverdine and pyochelin amongst others. This species expresses the ferrichrome receptor.[130] *P. fluorescens* is a fish pathogen,[131] and occasionally causes disease in humans with compromised immune systems.[132,133] In this work, QDs were coated with polyethyleneglycol-phosphoethanolamine (PEG-PD-QD) and ferrichrome was coupled to the terminal amino groups of PEG-PD-QD by using carbodiimide-based coupling chemistry. Incubation of the ferrichrome-QDs with cultures of *P. fluorescens* resulted in clustering and sedimentation observable by fluorescence microscopy and UV-visible spectroscopy. The clustering phenomenon was not observed when the ferrichrome-QDs were incubated with *Bacillus subtilis* or with *P. fluorescens* cultures that were pre-incubated with ferrichrome.

The last proof-of-concept approach employs an immobilized siderophore designed to separate siderophore-binding proteins from cell extracts and is applicable to pathogen detection (Figure 9). Motivated to provide a simple and direct method for the discovery of siderophore-binding proteins in cell extracts, a biotinylated derivative of petrobactin (**22**, B-petrobactin), a siderophore produced by marine bacteria[134] and the human pathogens *Bacillus cereus* and *Bacillus anthracis*,[135] was synthesized.[120] The ferric complex of B-petrobactin was incubated with streptavidin-agarose beads, which were used to prepare a petrobactin-affinity column. Following pre-treatment of the column with BSA to reduce non-specific binding. *B. subtilis* cell lysates were loaded onto the column and eluted with guanidinium chloride solution, and SDS-

PAGE analysis of eluted fractions revealed that only one protein was repeatedly retained on the column. Trypsin digest and mass spectrometry identified this protein as YclQ, an ABC transporter binding protein and member of the *ycl*NOPQ gene cluster. Prior work established that YclQ is the petrobactin-binding protein utilized by *B. subtilis* and that it coordinates apo and ferric petrobactin with K_d values of 32 and 142 nM, respectively (determined by fluorometric titration).[136] Indeed, the *B. subtilis* mutant Δ*yclQ* did not exhibit growth recovery following supplementation of nutrient-depleted growth medium with petrobactin whereas growth recovery was observed for the control strain. In agreement with the B-petrobactin pull-down assay, these data indicate that YclQ is the only petrobactin-binding protein expressed on the *B. subtilis* cell surface.

Although this approach was intended for the discovery of siderophore-binding proteins, its applicability to pathogen capture is clear and warrants careful consideration. Incubating bacterial samples with biotinylated siderophores and resin or magnetic beads bearing streptavidin affords a means to separate the bound and unbound cells. Moreover, the biotin/streptavidin interaction may be employed in other immobilization strategies. A biotinylated ferrichrome, prepared by chemical synthesis[137] and a biotinylated salmochelin, prepared by chemoenzymatic synthesis[138] have been reported in the chemical literature. Synthetic routes to other biotinylated siderophores, and biotin attachment strategies that do not compromise iron coordination or interaction with the target receptor, are required for this approach to be broadly applicable.

IV. Summary and Perspectives

This minireview summarizes advances in siderophore-based detection of iron and microbial pathogens reported through mid-2012. Building upon decades of fundamental studies in siderophore coordination chemistry, total synthesis and biology, some highlights of the past few years include reports of siderophore-based turn-on Fe(III) sensors and pathogen capture strategies. These proof-of-concept studies warrant further elaboration. Moreover, additional directions in both fundamental research and technology development with broad impact (i.e. environmental monitoring, therapeutics, diagnostics) exist. Along these lines, expanding the

toolbox of available siderophore scaffolds is an important step for advancing the field. Of ca. 500 siderophores isolated to date, only a handful have been evaluated in applications-based work. DFO, pyoverdine family members, and synthetic siderophore mimics are commonly employed because they are commercially available (i.e. DFO) or easily obtainable (i.e. pyoverdines), and afford relatively facile chemical modification. Limitations in siderophore availability may result from difficulties in cultivating the producer organism and/or isolating adequate quantities of the molecule in high purity from cultures. In addition, site-specific chemical modification of native siderophore platforms that house multiple functional groups is oftentimes challenging. Organic synthesis affords the means to circumvent these issues, and the total syntheses of many siderophores have been achieved. The synthetic routes to functionalized mycobactin,[48] petrobactin,[120] and pychelin[88] scaffolds reported in 2010-2011 provide opportunities for further elaboration. Chemoenzymatic and biosynthetic production of novel siderophores and siderophore conjugates are additional avenues worthy of exploration. Indeed, an artificial pathway to 3,4-dihydroxybenzoic acid was recently utilized to produce a novel catechol-derived aminocoumarin antibiotic in *Streptomycetes coelicolor* M512.[139]

From the standpoint of Fe(III) detection, additional photophysical characterization of fluorescent siderophores and fluorophore-siderophore conjugates is warranted. Standard characterization (i.e. quantum yield values and extinction coefficients for the apo and metal-bound species) is often lacking. In some instances, these values were determined in prior work and under conditions irrelevant to the sensing application. These data provide valuable quantitative information useful for making comparisons between molecules, and are generally required by other sensing fields. Lastly, more detailed mechanistic studies, especially for molecules that provide fluorescence enhancement with Fe(III) coordination, will afford valuable insights of broad relevance to the metal-ion sensing field and aid future sensor design.

Whether the proof-of-concept methods for pathogen capture and siderophore-protein discovery described above are applicable to pathogen detection in more complex biological and clinical samples remains to be evaluated. Testing in real-world samples is an important first step in this regard, and achieving the required sensitivity and selectivity will likely require optimization and new design strategies that include multiplexing. In closing, we aim for this minireview to

summarize highlights spanning approximately two decades of siderophore-based detection research, provide a helpful resource for the community, and catalyze new frontiers in siderophore-based research. We look forward to the outcomes of such future endeavors.

Acknowledgements The Department of Chemistry at MIT is gratefully acknowledged for financial support. We thank Eric Victor for assisting with the preparation of Figure 2.

References

1. C. Chen and B. H. Paw, *Biochim. Biophys. Acta*, 2012, doi:10.1016/j.bbamcr.2012.01.003.
2. V. Braun and K. Hantke, *Curr. Opin. Chem. Biol.*, 2011, **15**, 328-334.
3. T. Kobayashi and N. K. Nishizawa, *Annu. Rev. Plant Biol.*, 2012, **63**, 16.11-16.22.
4. T. Goswami, A. Rolfs and M. A. Hediger, *Biochem. Cell. Biol.*, 2002, **80**, 679-689.
5. K. Gkouvatsos, G. Papanikolaou and K. Pantopoulos, *Biochim. Biophys. Acta*, 2012, **1820**, 188-202.
6. K. N. Raymond, E. A. Dertz and S. S. Kim, *Proc. Natl. Acad. Sci. U. S. A.*, 2003, **100**, 3584-3588.
7. R. C. Hider and X. Kong, *Nat. Prod. Rep.*, 2010, **27**, 637-657.
8. M. Miethke and M. A. Marahiel, *Microbiol. Mol. Biol. Rev.*, 2007, **71**, 413-451.
9. A. Garenaux, M. Caza and C. M. Dozois, *Vet. Microbiol.*, 2011, **153**, 89-98.
10. C. P. Owens, J. Du, J. H. Dawson and C. W. Goulding, *Biochemistry*, 2012, **51**, 1518-1531.
11. N. D. Hammer and E. P. Skaar, *Annu. Rev. Microbiol.*, 2011, **65**, 129-147.
12. T. F. Moraes, R. H. Yu, N. C. J. Strynadka and A. B. Schryvers, *Mol. Cell*, 2009, **35**, 523-533.
13. C. Calmettes, J. Alcantara, R. H. Yu, A. B. Schryvers and T. F. Moraes, *Nat. Struct. Mol. Biol.*, 2012, **19**, 358-360.
14. M. Nairz, A. Schroll, T. Sonnweber and G. Weiss, *Cell. Microbiol.*, 2010, **12**, 1691-1702.
15. M. Caza, F. Lépine and C. M. Dozois, *Mol. Microbiol.*, 2011, **80**, 266-282.

16. M. L. V. Crouch, M. Castor, J. E. Karlinsey, T. Kalhorn and F. C. Fang, *Mol. Microbiol.*, 2008, **67**, 971-983.
17. A. M. Albrecht-Gary and A. L. Crumbliss, *Met. Ions in Biol. Syst.*, 1998, **35**, 239-327.
18. A. L. Crumbliss and J. M. Harrington, *Adv. Inorg. Chem.*, 2009, **61**, 179-250.
19. J. Francis, J. Madinaveitia, H. M. Macturk and G. A. Snow, *Nature*, 1949, **163**, 365-366.
20. S. Dhungana, P. S. White and A. L. Crumbliss, *J. Biol. Inorg. Chem.*, 2001, **6**, 810-818.
21. D. Van der Helm, J. R. Baker, D. L. Eng-Wilmot, M. B. Hossain and R. A. Loghry, *J. Am. Chem. Soc.* , 1980, **102**, 4224-4231.
22. M. C. Miller, S. Parkin, J. D. Fetherston, R. D. Perry and E. Demoll, *J. Inorg. Biochem.*, 2006, **100**, 1495-1500.
23. T. B. Karpishin and K. N. Raymond, *Angew. Chem. Int. Ed.*, 1992, **31**, 466-468.
24. J. H. Crosa and C. T. Walsh, *Microbiol. Mol. Biol. Rev.*, 2002, **66**, 223-249.
25. S. M. Barry and G. L. Challis, *Curr. Opin. Chem. Biol.*, 2009, **13**, 205-215.
26. M. A. Fischbach and C. T. Walsh, *Chem. Rev.*, 2006, **106**, 3468-3496.
27. E. S. Sattely, M. A. Fischbach and C. T. Walsh, *Nat. Prod. Rep.*, 2008, **25**, 757-793.
28. R. Chakraborty, E. Storey and D. van der Helm, *Biometals*, 2007, **20**, 263-274.
29. V. Braun and F. Endriss, *Biometals*, 2007, **20**, 219-231.
30. K. D. Krewulak and H. J. Vogel, *Biochim. Biophys. Acta. Biomembr.*, 2008, **1778**, 1781-1804.
31. T. J. Silhavy, D. Kahne and S. Walker, *Cold Spring Harb. Perspect. Biol.*, 2010, **2**: a1000414.
32. K. D. Krewulak and H. J. Vogel, *Biochem. Cell. Biol.*, 2011, **89**, 87-97.
33. K. Postle and R. A. Larsen, *Biometals*, 2007, **20**, 453-465.
34. F. C. Beasley, E. D. Vines, J. C. Grigg, Q. Zheng, S. Y. Liu, G. A. Lajoie, M. E. P. Murphy and D. E. Heinrichs, *Mol. Microbiol.*, 2009, **72**, 947-963.
35. A. Bagg and J. B. Neilands, *Microbiol. Rev.*, 1987, **51**, 509-518.
36. A. Bagg and J. B. Neilands, *Biochemistry*, 1987, **26**, 5471-5477.
37. P. V. Bernhardt, *Dalton Trans.*, 2007, 3214-3220.
38. H. Nick, *Curr. Opin. Chem. Biol.*, 2007, **11**, 419-423.

39. Y. Yu, J. Wong, D. B. Lovejoy, D. S. Kalinowski and D. R. Richardson, *Clin. Cancer Res.*, 2006, **12**, 6876-6883.

40. G. J. Kontoghiorghes, A. Efstathiou, S. Loannou-Loucaides and A. Kolnagou, *Hemoglobin*, 2008, **32**, 217-227.

41. C. Ji, R. E. Juarez-Hernandez and M. J. Miller, *Future Med. Chem.*, **4**, 297-313.

42. V. Braun, *Drug Resist. Update*, 1999, **2**, 363-369.

43. V. Braun, A. Pramanik, T. Gwinner, M. Koberle and E. Bohn, *Biometals*, 2009, **22**, 3-13.

44. H. Budzikiewicz, *Curr. Top. Med. Chem.*, 2001, **1**, 73-82.

45. J. M. Roosenberg, 2nd, Y. M. Lin, Y. Lu and M. J. Miller, *Curr. Med. Chem.*, 2000, **7**, 159-197.

46. M. Ballouche, P. Cornelis and C. Baysse, *Recent Pat. Anti-infect. Drug Discovery*, 2009, **4**, 190-205.

47. U. Möllmann, L. Heinisch, A. Bauernfeind, T. Kohler and D. Ankel-Fuchs, *Biometals*, 2009, **22**, 615-624.

48. M. J. Miller, A. J. Walz, H. Zhu, C. Wu, G. Moraski, U. Mollmann, E. M. Tristani, A. L. Crumbliss, M. T. Ferdig, L. Checkley, R. L. Edwards and H. I. Boshoff, *J. Am. Chem. Soc.*, 2011, **133**, 2076-2079.

49. E. L. Que, D. W. Domaille and C. J. Chang, *Chem. Rev.*, 2008, **108**, 4328-4328.

50. E. M. Nolan and S. J. Lippard, *Chem. Rev.*, 2008, **108**, 3443-3480.

51. A. P. de Silva, T. S. Moody and G. D. Wright, *Analyst*, 2009, **134**, 2385-2393.

52. B. P. Espósito, S. Epsztejn, W. Breuer and Z. I. Cabantchik, *Anal. Biochem.*, 2002, **304**, 1-18.

53. O. Kakhlon and Z. I. Cabantchik, *Free Radical Biol. Med.*, 2002, **33**, 1037-1046.

54. D. D. Doorneweerd, W. A. Henne, R. G. Reifenberger and P. S. Low, *Langmuir*, 2010, **26**, 15424-15429.

55. Y. Kim, D. P. Lyvers, A. Wei, R. G. Reifenberger and P. S. Low, *Lab Chip*, 2012, **12**, 971-976.

56. S. M. Wu, Z. L. Zhang, X. D. Wang, M. X. Zhang, J. Peng, Z. X. Xie and D. W. Pang, *J. Phys. Chem. C*, 2009, **113**, 9169-9174.

57. T. Manning, G. Kean, J. Thomas, K. Thomas, M. Corbitt, D. Gosnell, R. Ware, S. Fulp, J. Jarrard and D. Phillips, *Curr. Med. Chem.*, 2009, **16**, 2416-2429.

58. M. J. Miller, H. Zhu, Y. Xu, C. Wu, A. J. Walz, A. Vergne, J. M. Roosenberg, G. Moraski, A. A. Minnick, J. McKee-Dolence, J. Hu, K. Fennell, E. Kurt Dolence, L. Dong, S. Franzblau, F. Malouin and U. Möllmann, *Biometals*, 2009, **22**, 61-75.

59. A. Shanzer, J. Libman, S. D. Lytton, H. Glickstein and Z. I. Cabantchik, *Proc. Natl. Acad. Sci. U. S. A.*, 1991, **88**, 6585-6589.

60. S. J. Rodgers, C. W. Lee, C. Y. Ng and K. N. Raymond, *Inorg. Chem.*, 1987, **26**, 1622-1625.

61. D. J. Ecker, L. D. Loomis, M. E. Cass and K. N. Raymond, *J. Am. Chem. Soc.*, 1988, **110**, 2457-2464.

62. M. Meyer, J. R. Telford, S. M. Cohen, D. J. White, J. Xu and K. N. Raymond, *J. Am. Chem. Soc.*, 1997, **119**, 10093-10103.

63. S. Zürcher, D. Wäckerlin, Y. Bethuel, B. Malisova, M. Textor, S. Tosatti and K. Gademann, *J. Am. Chem. Soc.*, 2006, **128**, 1064-1065.

64. E. Franzmann, F. Khalil, C. Weidmann, M. Schröder, M. Rohnke, J. Janek, B. M. Smarsly and W. Maison, *Chem. Eur. J.*, 2011, **17**, 8596-8603.

65. H. Weizman, O. Ardon, B. Mester, J. Libman, O. Dwir, Y. Hadar, Y. Chen and A. Shanzer, *J. Am. Chem. Soc.*, 1996, **118**, 12368-12375.

66. F. Fages, B. Bodenant and T. Weil, *J. Org. Chem.*, 1996, **61**, 3956-3961.

67. O. Ardon, R. Nudelman, C. Caris, J. Libman, A. Shanzer, Y. N. Chen and Y. Hadar, *J. Bacteriol.*, 1998, **180**, 2021-2026.

68. R. Nudelman, O. Ardon, Y. Hadar, Y. N. Chen, J. Libman and A. Shanzer, *J. Med. Chem.*, 1998, **41**, 1671-1678.

69. H. Ouchetto, M. Dias, R. Mornet, E. Lesuisse and J. M. Camadro, *Bioorg. Med. Chem.*, 2005, **13**, 1799-1803.

70. R. Kikkeri, H. Traboulsi, N. Humbert, E. Gumienna-Kontecka, R. Arad-Yellin, G. Melman, M. Elhabiri, A. M. Albrecht-Gary and A. Shanzer, *Inorg. Chem.*, 2007, **46**, 2485-2497.

71. N. Singh, N. Kaur and J. F. Callan, *J. Fluoresc.*, 2009, **19**, 649-654.

72. N. C. Lim, S. V. Pavlova and C. Brückner, *Inorg. Chem.*, 2009, **48**, 1173-1182.

73. T. Palanché, F. Marmolle, M. A. Abdallah, A. Shanzer and A. M. Albrecht-Gary, *J. Biol. Inorg. Chem.*, 1999, **4**, 188-198.

74. T. Palanché, S. Blanc, C. Hennard, M. A. Abdallah and A. M. Albrecht-Gary, *Inorg. Chem.*, 2004, **43**, 1137-1152.

75. M. Sharma, R. Saxena and N. K. Gohil, *Anal. Biochem.*, 2009, **394**, 186-191.

76. J. M. Barrero, M. C. Morenobondi, M. C. Pérez-Conde and C. Cámara, *Talanta*, 1993, **40**, 1619-1623.

77. P. Pulido-Tofiño, J. M. Barrero-Moreno and M. C. Pérez-Conde, *Talanta*, 2000, **51**, 537-545.

78. M. Mureseanu, G. Renard, A. Galarneau and D. A. Lerner, *Talanta*, 2003, **60**, 515-522.

79. G. Renard, M. Mureseanu, A. Galarneau, D. A. Lerner and D. Brunel, *New J. Chem.*, 2005, **29**, 912-918.

80. T. Panadda, C. Worakarn, C. Saksit and R. Chalerm, *J. Environ. Sci. China*, 2009, **21**, 1009-1016.

81. J. M. Barrero, C. Cámara, M. C. Pérez-Conde, C. San José and L. Fernández, *Analyst*, 1995, **120**, 431-435.

82. C. K. S. C. C. Lam, T. D. Jickells, D. J. Richardson and D. A. Russell, *Anal. Chem.*, 2006, **78**, 5040-5045.

83. M. F. Yoder and W. S. Kisaalita, *J. Biol. Eng.*, 2011, **5**, 1-12.

84. S. D. Lytton, Z. I. Cabantchik, J. Libman and A. Shanzer, *Mol. Pharmacol.*, 1991, **40**, 584-590.

85. E. Barness, Y. Hadar, Y. Chen, A. Shanzer and J. Libman, *Plant Physiol.*, 1992, **99**, 1329-1335.

86. B. L. Su, N. Moniotte, N. Nivarlet, L. H. Chen, Z. Y. Fu, J. Desmet and J. Li, *J. Colloid. Interface Sci.*, 2011, **358**, 136-145.

87. Y. Ye, S. Bloch, B. Xu and S. Achilefu, *Bioconjugate Chem.*, 2008, **19**, 225-234.

88. S. Noël, L. Guillon, I. J. Schalk and G. L. A. Mislin, *Organic Lett.*, 2011, **13**, 844-847.

89. K. M. Orcutt, W. S. Jones, A. McDonald, D. Schrock and K. J. Wallace, *Sensors*, 2010, **10**, 1326-1337.

90. D. Mossialos and G. D. Amoutzias, *Future Microbiol.* , 2007, **2**, 387-395.

91. J. Ravel and P. Cornelis, *Trends Microbiol.*, 2003, **11**, 195-200.

92. H. Boukhalfa, S. D. Reilly, R. Michalczyk, S. Iyer and M. P. Neu, *Inorg. Chem.*, 2006, **45**, 5607-5616.

93. O. Knosp, M. Vontigerstrom and W. J. Page, *J. Bacteriol.*, 1984, **159**, 341-347.

94. P. Demange, A. Bateman, A. Dell and M. A. Abdallah, *Biochemistry*, 1988, **27**, 2745-2752.

95. S. Namiranian, D. J. Richardson, D. A. Russell and J. R. Sodeau, *Photochem. Photobiol.*, 1997, **65**, 777-782.

96. A. E. Tindale, M. Mehrotra, D. Ottem and W. J. Page, *Microbiology (U. K.)*, 2000, **146**, 1617-1626.

97. M. Sharma and N. K. Gohil, *Eng. Life Sci.*, 2010, **10**, 304-310.

98. W. Breuer, M. J. J. Ermers, P. Pootrakul, A. Abramov, C. Hershko and Z. I. Cabantchik, *Blood*, 2001, **97**, 792-798.

99. W. Breuer and Z. I. Cabantchik, *Anal. Biochem.*, 2001, **299**, 194-202.

100. A. M. Albrecht-Gary, S. Blanc, N. Rochel, A. Z. Ocaktan and M. Abdallah, *Inorg. Chem.*, 1994, **33**, 6391-6402.

101. R. J. Bergeron, J. B. Dionis, G. T. Elliott and S. J. Kline, *J. Biol. Chem.*, 1985, **260**, 7936-7944.

102. B. A. Bergquist, J. Wu and E. A. Boyle, *Geochim. Cosmochim. Acta*, 2007, **71**, 2960-2974.

103. Y. P. Ye, S. Bloch and S. Achilefu, *Optics in Health Care and Biomedical Optics Iii*, 2008, **6826**, U278-U286.

104. S. Noël, V. Gasser, B. Pesset, F. Hoegy, D. Rognan, I. J. Schalk and G. L. A. Mislin, *Org. Biomol. Chem.*, 2011, **9**, 8288-8300.

105. R. Sjöback, J. Nygren and M. Kubista, *Spectrocim. Acta Part A*, 1995, **51**, L7-L21.

106. C. D. Cox and R. Graham, *J. Bacteriol.*, 1979, **137**, 357-364.

107. C. D. Cox, K. L. Rinehart, M. L. Moore and J. C. Cook, *Proc. Natl. Acad. Sci. U. S. A.*, 1981, **78**, 4256-4260.

108. J. Brandel, N. Humbert, M. Elhabiri, I. J. Schalk, G. L. A. Mislin and A. M. Albrecht-Gary, *Dalton Trans.*, 2012, **41**, 2820-2834.

109. P. Visca, G. Colotti, L. Serino, D. Verzili, N. Orsi and E. Chiancone, *App. Environ. Microbiol.*, 1992, **58**, 2886-2893.

110. R. K. Jackson, Y. Shi, X. D. Yao and S. C. Burdette, *Dalton Trans.*, 2010, **39**, 4155-4161.

111. D. P. Kennedy, C. M. Kormos and S. C. Burdette, *J. Am. Chem. Soc.*, 2009, **131**, 8578-8586.

112. H. X. Wang, D. L. Wang, Q. Wang, X. Y. Li and C. A. Schalley, *Org. Biomol. Chem.*, 2010, **8**, 1017-1026.

113. G. J. He, Y. G. Zhao, C. He, Y. Liu and C. Y. Duan, *Inorg. Chem.*, 2008, **47**, 5169-5176.

114. Y. M. You, E. Tomat, K. Hwang, T. Atanasijevic, W. Nam, A. P. Jasanoff and S. J. Lippard, *Chem. Commun.*, 2010, **46**, 4139-4141.

115. O. Kotova, S. Comby and T. Gunnlaugsson, *Chem. Commun.*, 2011, **47**, 6810-6812.

116. B. J. Hernlem, L. M. Vane and G. D. Sayles, *Wat. Res.*, 1999, **33**, 951-960.

117. J. R. Brainard, B. A. Strietelmeier, P. H. Smith, P. J. Langstonunkefer, M. E. Barr and R. R. Ryan, *Radiochim. Acta*, 1992, **58-9**, 357-363.

118. S. M. Kraemer, J. D. Xu, K. N. Raymond and G. Sposito, *Environ. Sci. Technol.*, 2002, **36**, 1287-1291.

119. K. Binnemans, *Chem. Rev.*, 2009, **109**, 4283-4374.

120. N. Bugdahn, F. Peuckert, A. G. Albrecht, M. Miethke, M. A. Marahiel and M. Oberthür, *Angew. Chem. Int. Ed.*, 2010, **49**, 10210-10213.

121. S. K. Buchanan, B. S. Smith, L. Venkatramani, D. Xia, L. Esser, M. Palnitkar, R. Chakraborty, D. van der Helm and J. Deisenhofer, *Nat. Struct. Biol.*, 1999, **6**, 56-63.

122. P. D. Pawelek, N. Croteau, C. Ng-Thow-Hing, C. M. Khursigara, N. Moiseeva, M. Allaire and J. W. Coulton, *Science*, 2006, **312**, 1399-1402.

123. D. Cobessi, H. Celia, N. Folschweiller, I. J. Schalk, M. A. Abdallah and F. Pattus, *J. Mol. Biol.*, 2005, **347**, 121-134.

124. E. Clément, P. J. Mesini, F. Pattus and I. J. Schalk, *Biochemistry*, 2004, **43**, 7954-7965.

125. F. O. Hoegy, H. Celia, G. L. Mislin, M. Vincent, J. Gallay and I. J. Schalk, *J. Biol. Chem.*, 2005, **280**, 20222-20230.

126. N. Folschweiller, J. Gallay, M. Vincent, M. A. Abdallah, F. Pattus and I. J. Schalk, *Biochemistry*, 2002, **41**, 14591-14601.

127. A. J. Bäumler and K. Hantke, *Mol. Microbiol.*, 1992, **6**, 1309-1321.

128. A. J. Bäumler and K. Hantke, *J. Bacteriol.*, 1992, **174**, 1029-1035.

129. P. W. Abcarian and B. E. Demas, *Am. J. Roentgenol.*, 1991, **157**, 773-775.

130. I. T. Paulsen, C. M. Press, J. Ravel, D. Y. Kobayashi, G. S. A. Myers, D. V. Mavrodi, R. T. DeBoy, R. Seshadri, Q. H. Ren, R. Madupu, R. J. Dodson, A. S. Durkin, L. M. Brinkac, S. C. Daugherty, S. A. Sullivan, M. J. Rosovitz, M. L. Gwinn, L. W. Zhou, D. J. Schneider, S. W. Cartinhour, W. C. Nelson, J. Weidman, K. Watkins, K. Tran, H. Khouri, E. A. Pierson, L. S. Pierson, L. S. Thomashow and J. E. Loper, *Nature Biotechnol.*, 2005, **23**, 873-878.

131. W.-W. Zhang, Y.-H. Hu, H.-L. Wang and L. Sun, *Vet. Microbiol.*, 2009, **139**, 183-188.

132. P.-R. Hsueh, L.-J. Teng, H.-J. Pan, Y.-C. Chen, C.-C. Sun, S.-W. Ho and K.-T. Luh, *J. Clin. Microbiol.*, 1998, **36**, 2914-2917.

133. A. Madi, O. Lakhdari, H. M. Blottière, M. Guyard-Nicodème, K. Le Roux, A. Groboillot, P. Svinareff, J. Doré, N. Orange, M. G. J. Feuilloley and N. Connil, *Bmc Microbiol.*, 2010, **10**.

134. A. Butler, *Biometals*, 2005, **18**, 369-374.

135. M. K. Wilson, R. J. Abergel, K. N. Raymond, J. E. Arceneaux and B. R. Byers, *Biochem. Biophys. Res. Commun.*, 2006, **348**, 320-325.

136. A. M. Zawadzka, Y. Kim, N. Maltseva, R. Nichiporuk, Y. Fan, A. Joachimiak and K. N. Raymond, *Proc. Natl. Acad. Sci. U. S. A.*, 2009, **106**, 21854-21859.

137. Y. M. Lin and M. J. Miller, *J. Org. Chem.*, 1999, **64**, 7451-7458.

138. E. M. Nolan and C. T. Walsh, *Biochemistry*, 2008, **47**, 9289-9299.

139. S. Alt, N. Burkard, A. Kulik, S. Grond and L. Heide, *Chem. Biol.*, 2011, **18**, 304-313.

140. R. D. Perry, P. B. Balbo, H. A. Jones, J. D. Fetherston, and E. DeMoll, *Microbiol.* **1999,** *145*, 1181-1190.

141. G. Schwarzenbach and K. Schwarzenbach, *Helv. Chim. Acta.,* 1963**, 46** , 1390-1400.

142. G. B. Wong, M. J. Kappel, K. N. Raymond, B. Matzanke, and G. Winkelmann, *J. Am. Chem. Soc.* 1983**, 105**, 810-815.

143. G. Anderegg, F. L'Eplattenier, and G. Schwarzenbach, *Helv. Chim. Acta* 1963, **46**, 1409-1422.

144. L. D. Loomis and K. N. Raymond, *Inorg. Chem.* 1991, **30**, 906-911.

145. G. Zhang, S. A. Amin, F. C. Küpper, P. D. Holt, C. J. Carrano, and A. Butler, *Inorg. Chem.* 2009, **48**, 11466-11473.

146. H. J. Maccordick, J. J. Schleiffer, and G. Duplatre, *Radiochim. Acta* 1985, **38**, 43-47.

Table 1. Properties of select siderophores produced by bacteria and fungi.

No.	Siderophore	Producing Organism(s)[a]	logK_f (Fe^{III})[b]	p[Fe^{III}][c]	Naturally emissive	Ref[d]
1	Pyoverdine	*Pseudomonas* spp.	30.8	27	yes	100
2	Pyochelin	*Pseudomonas aeruginosa, Burkholderia cepacia*	5.4, 17.2[e]	16.0	yes	106, 108
3	Azotobactin ð	*Azotobacter vinelandii*	28.1	27.8	yes	74
4	Yersiniabactin	*Yersinia enterocolitica, Yersinia pestis*	36.6	n.d.	yes	140
5	Desferrioxamine B	*Nocardia* spp., *Streptomyces* spp.	30.6	26.6	no	141
6	Ferrichrome	*Aspergillus* spp., *Penicillium* spp., *Ustilago* spp.	29.1	25.2	no	142, 143
7	Enterobactin	*Klebisella* spp., *Enterobacter* spp., *Erwinia* spp.	49	35.5	no	144
8	Parabactin	*Paracoccus denitrificans*	~48	n.d.[f]	yes	101
9	Petrobactin	*Marinobacter hydrocarbonoclasticus, Bacillus cereus, Bacillus anthracis*	43	23.1	no	145
10	Mycobactin S	*Mycobacterium smegmatis*	26.6	n.d.[f]	no	146
11	Staphyloferrin B	*Staphylococcus hyicus*	n.d.[f]	n.d.[f]	no	

[a] Select examples of producing organisms. [b] K_f is the apparent forming constant of Fe^{III} and the fully deprotonated ligand. [c] When $[Fe^{III}]_{total} = 10^{-6}$ M, $[L]_{total} = 10^{-5}$ M, at pH 7.4. [d] The references specify the source of the stability constant. [e] The first value was determined in methanol due to the low solubility of the siderophore. The second value was determined in 20% ethanol/water. [f] n.d. = not determined.

Figure Captions

Figure 1. Examples of siderophores produced by Gram-negative bacteria (**1**-**5, 7-10**), Gram-positive bacteria (**11**) and fungi (**6**). The iron-coordinating moieties are highlighted in red. Multiple structural variants of some siderophores exist (i.e. pyoverdines, azotobactins, desferrioxamines, mycobactins, etc.). In such cases, one example is provided and referred to throughout the text unless noted otherwise.

Figure 2. Structures of ferrioxamine B (ref. 20), [Fe(ferrichrome)] (ref. 21), $[Fe(yersiniabactin)]^-$ (ref. 22) and $[V(enterobactin)]^{2-}$ (ref. 23) determined by X-ray crystallographic analysis. The oxygen atoms are depicted in red, the nitrogen atoms in blue, the sulfur atoms in yellow, and the carbon atoms in grey. The metal ions are labeled in green and the hydrogen atoms are omitted for clarity.

Figure 3. Immobilization of ferrioxamine B onto glycidoxy-grafted silica gel (ref. 79).

Figure 4. Structures of NBD- and fluorescein-containing fluorophore-DFO conjugates **12-14.** The donor atoms are depicted in red and the fluorophores are labeled in blue.

Figure 5. Structures of cypate-DFO conjugates **15-16** designed for cancer imaging studies. The donor atoms are depicted in red and the cypate fluorophores are labeled in blue.

Figure 6. Structure of pyochelin-NBD conjugates **17-18** that give fluorescence turn-on with Fe(III) coordination in aqueous solution. The donor atoms are depicted in red and the NBD fluorophores are labeled blue.

Figure 7. Iron detection based on lanthanide displacement. Molecules **19** and **20** exhibit terbium luminescence, which is quenched following Fe(III)-mediated Tb(III) displacement. The *N*-methylanthranyl moiety is depicted in blue.

Figure 8. Pathogen detection using siderophore-immobilization on glass chips (refs. 54 and 55). (A) Application of the siderophore-BSA conjugate to a PDMS stamp. (B) Immobilization of siderophore-BSA onto a gold-plated glass chip. (C) Exposure of the chip to a bacterial culture. (D) Imaging of bacterial capture.

Figure 9. (A) Isolation of siderophore-binding proteins by using biotin-siderophore conjugates (ref. 120). (B) Structure of biotinylated petrobactin **22**. The donor atoms are depicted in red and the biotin moiety is labeled in blue.

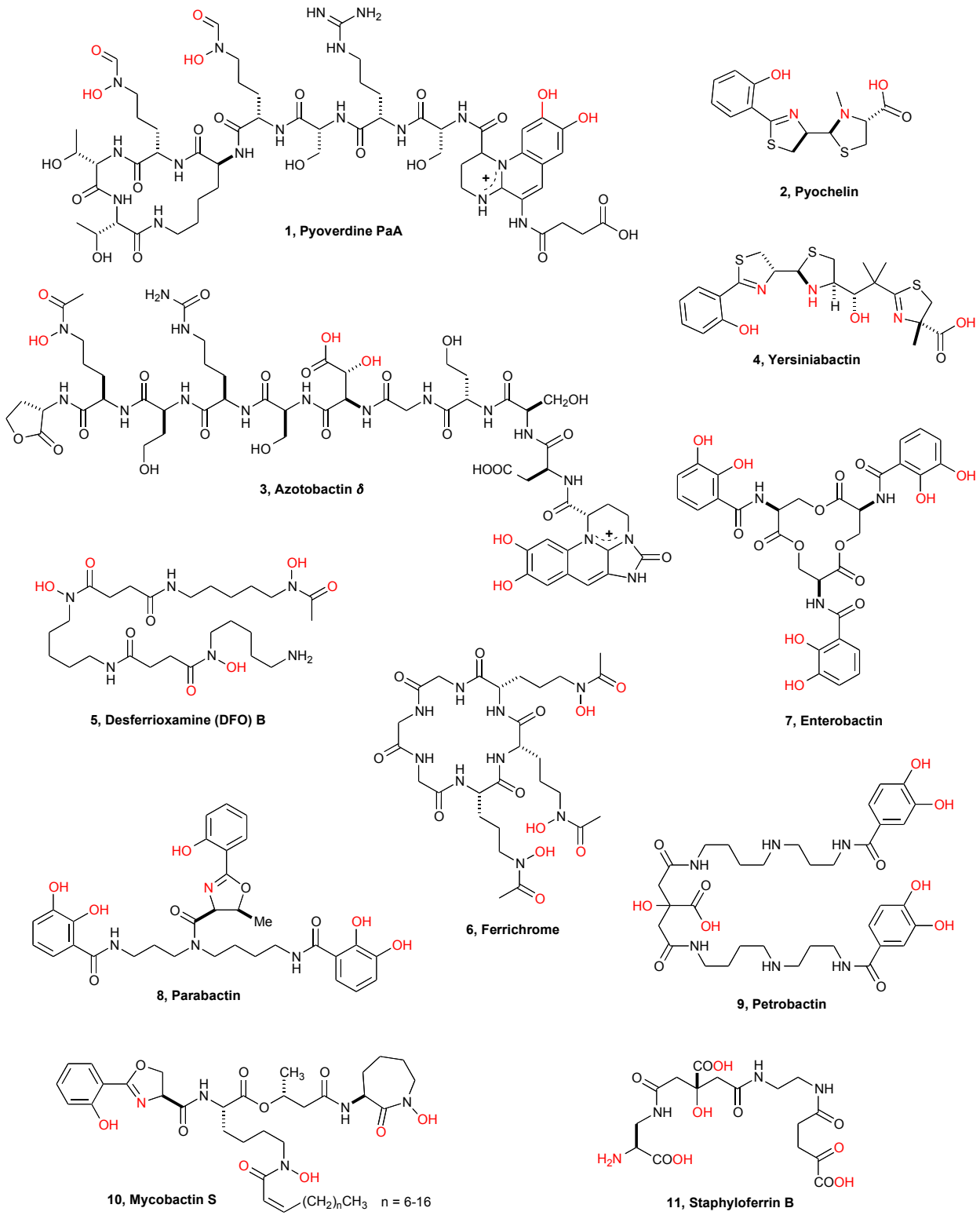

Figure 1. Zheng & Nolan (two columns)

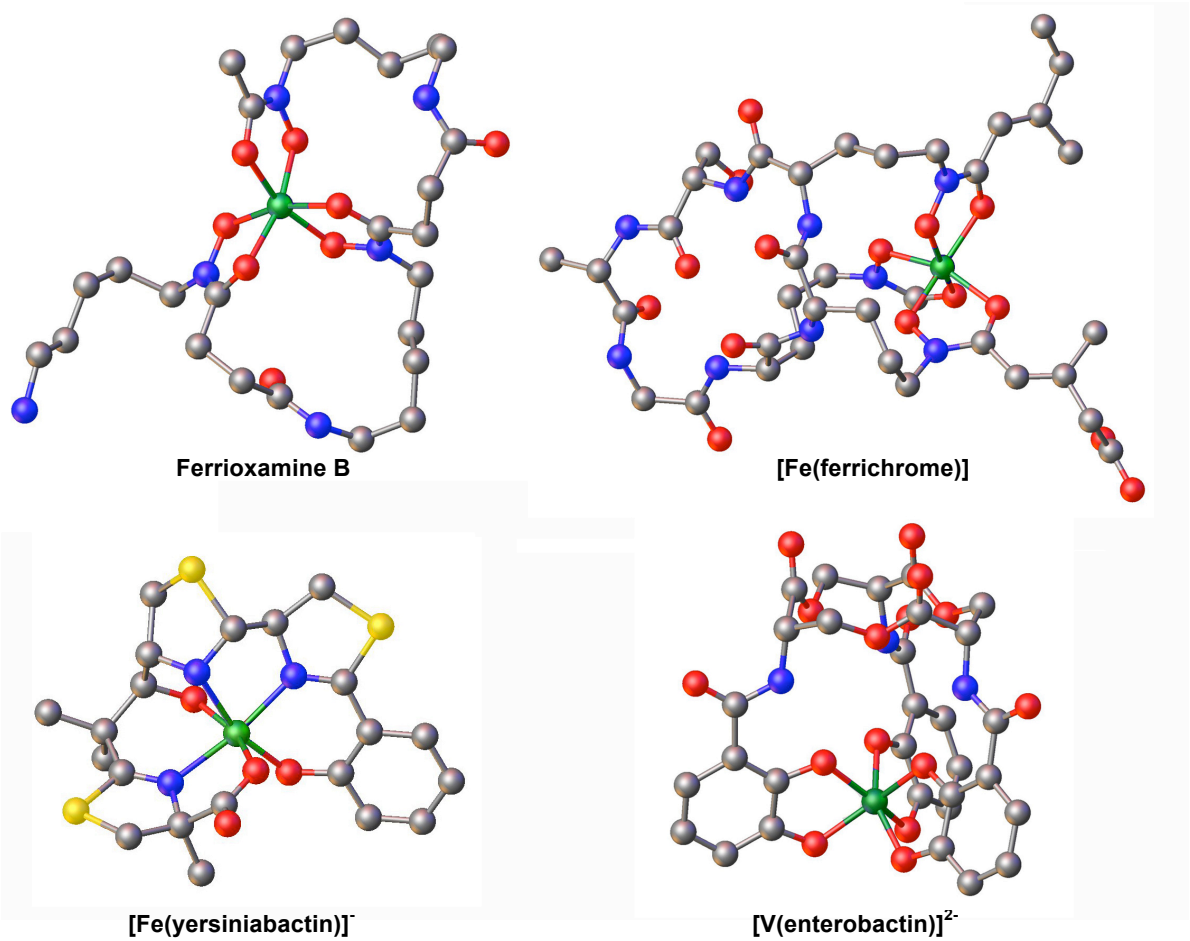

Figure 2. Zheng & Nolan (two columns)

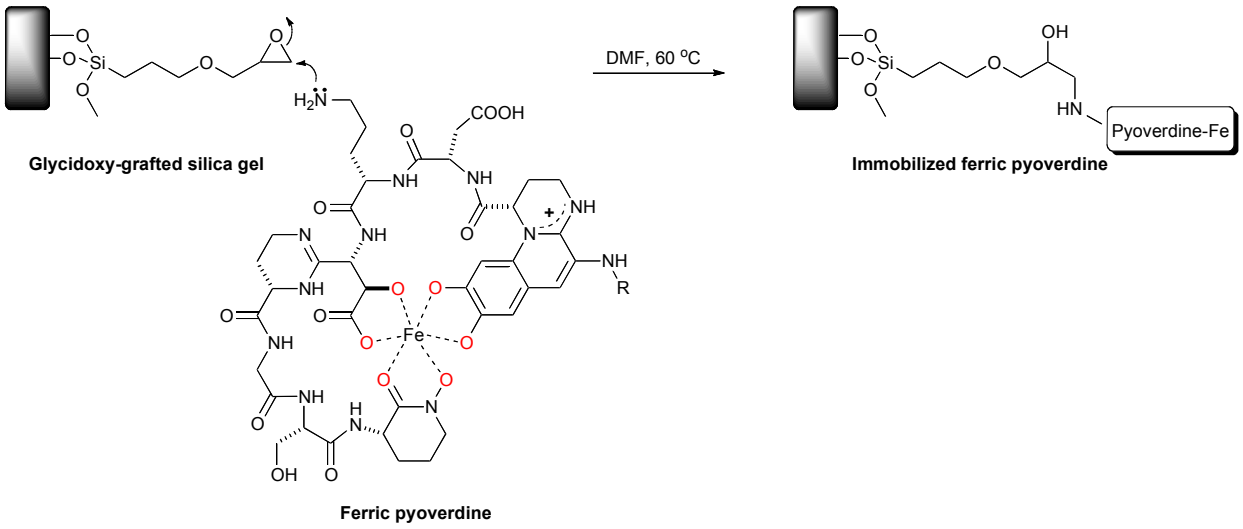

Figure 3. Zheng & Nolan (two columns)

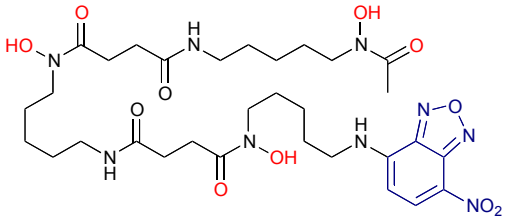

12, NBD-DFO

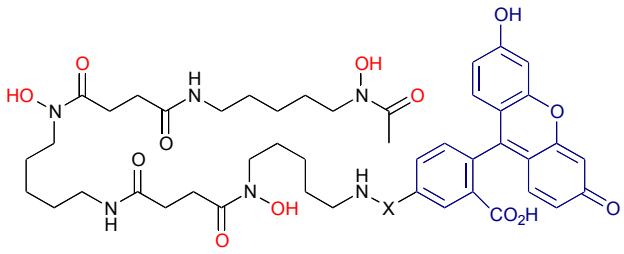

13, FL-DFO$_{thio}$ X =

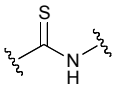

14, FL-DFO$_{am}$ X =

Figure 4. Zheng & Nolan (one column)

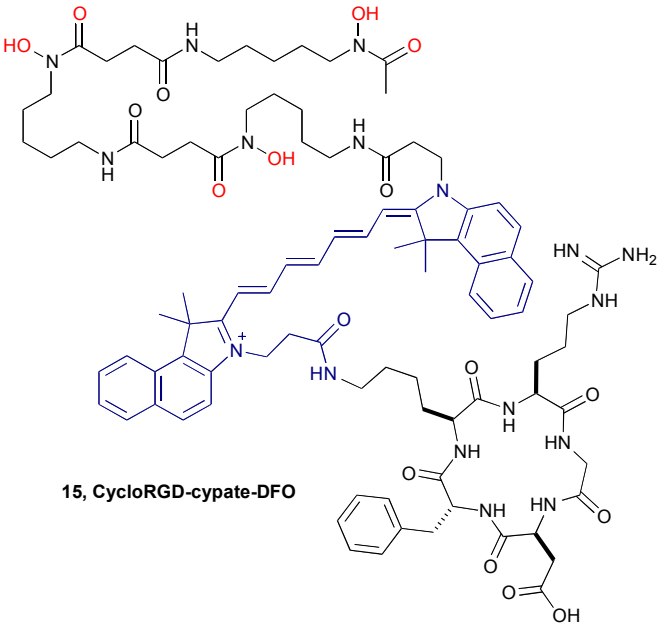

15, CycloRGD-cypate-DFO

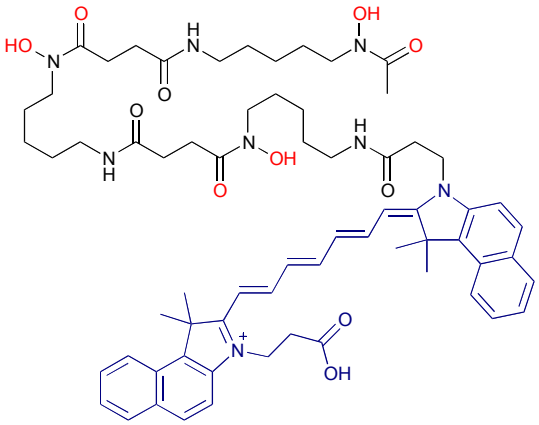

16, Cypate-DFO

Figure 5. Zheng & Nolan (two columns)

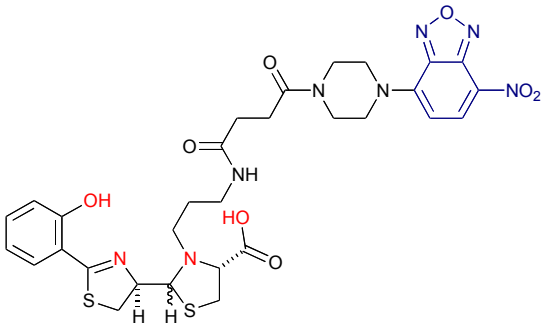

17, Pyochelin-NBD 1

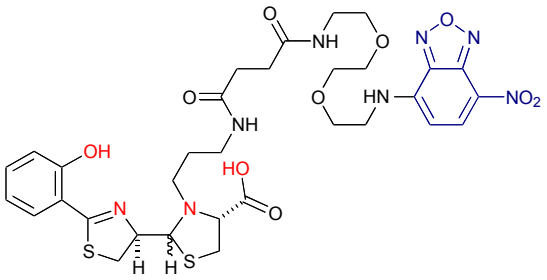

18, Pyochelin-NBD 2

Figure 6. Zheng & Nolan (one column)

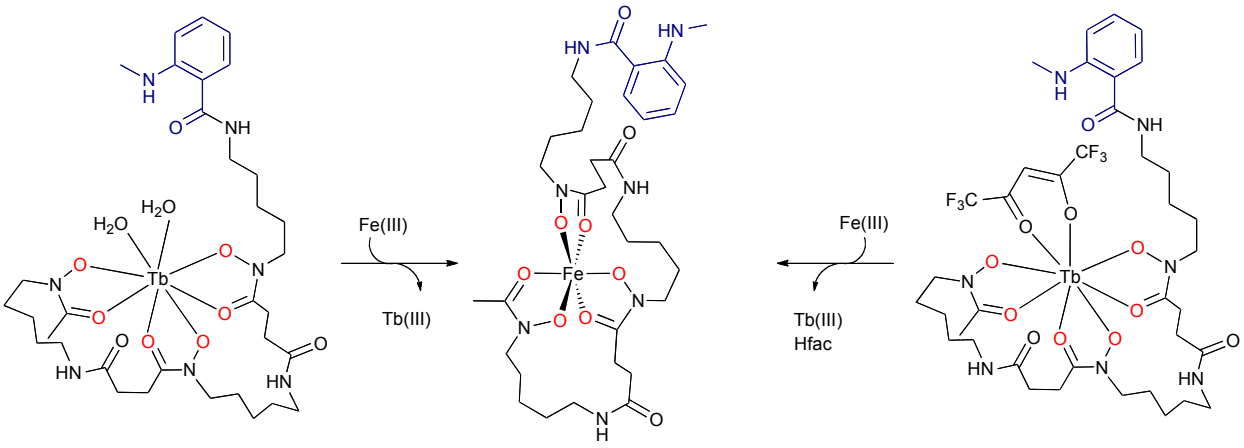

19
Tb(III) emission observed

21
Tb(III) emission quenched

20
Tb(III) emission observed
(water-compatible)

Figure 7. Zheng & Nolan (2 columns)

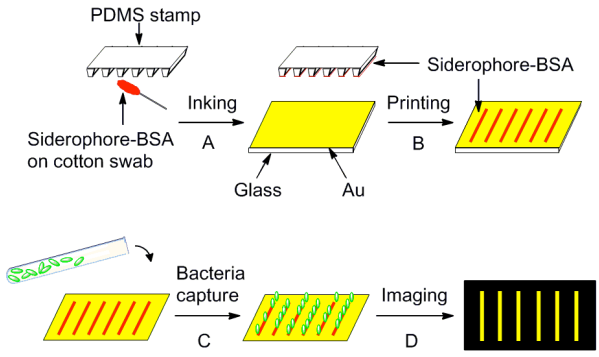

Figure 8. Zheng & Nolan (one column)

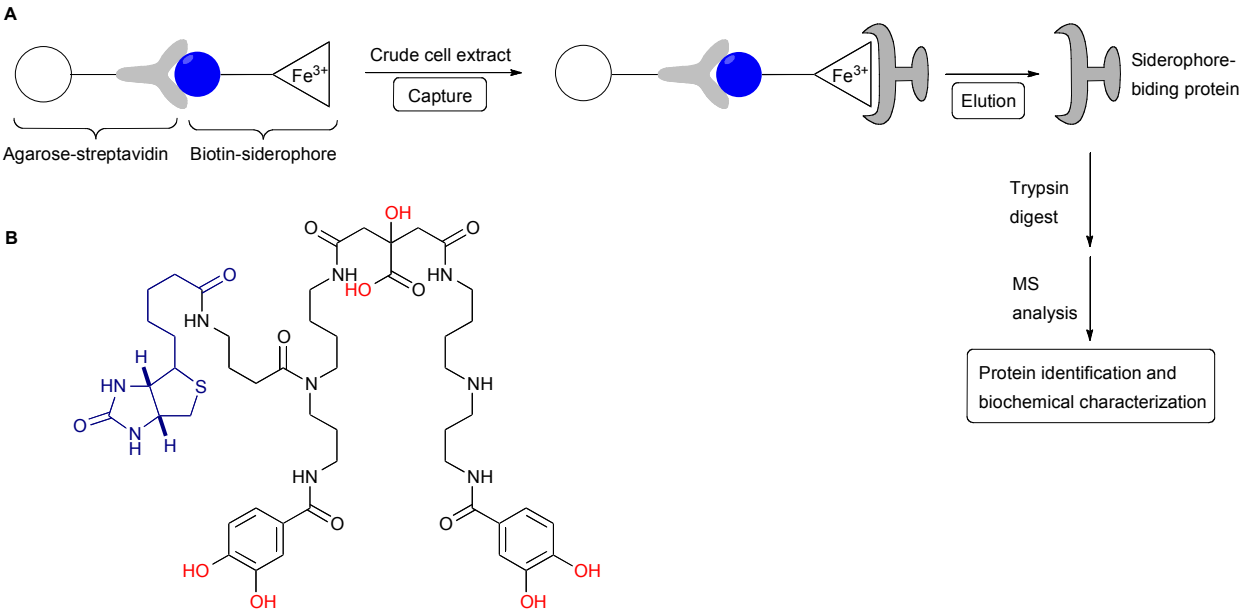

22, Biotin-petrobactin conjugate (B-petrobactin)

Figure 9. Zheng & Nolan (two columns)

TOC Graphic and Text

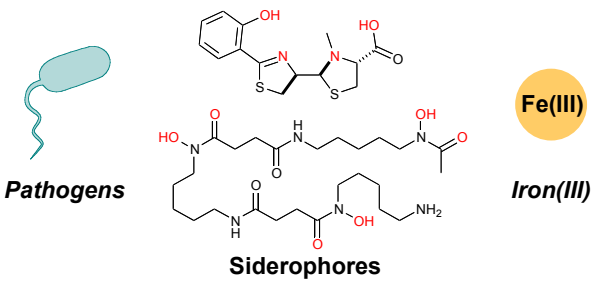

This minireview summarizes siderophore-based methods for the fluorescence detection of Fe(III) and capture of bacterial pathogens.